Continuous Steering-Function Control of Robot Carts

WINSTON L. NELSON, MEMBER, IEEE

Abstract—**The paths followed by automatically guided vehicles (AGV's) are generally made up of line and circular arc segments. For most AGV's, the steering functions required to keep the position and heading of the cart continuously aligned with such paths will have discontinuities at the line-arc-line transition points because the curvature of the path is discontinuous at these points. Since carts have inertia and limited steering forces, tracking errors are the inevitable result. Discussed in this paper are three alternative approaches for eliminating steering discontinuities: (1) changing the steering mechanism, (2) changing the guide-point on the cart, or (3) changing the curves on the path. The first approach requires a steering mechanism that moves the cart in any direction without changing its heading. Two such mechanisms exist, but possibly because of cost, performance, or reliability considerations, they have not yet found wide acceptance. The most common configurations in AGV's today are the steered-wheel types and differential-drive types. The second approach may be a reasonable choice for differential-drive carts but less so for steered-wheel carts because of their limited maneuverability. For applications where the third approach is preferred, two types of curves providing continuous steering functions for both steered-wheel and differential-drive carts are proposed: cartesian quintics for lane changes and polar splines for symmetric turns of arbitrary-angle. These curves have computationally simple, closed-form expressions that provide continuous curvature and precise matching of the boundary conditions at the line-curve junctions on the paths.**

I. Introduction

THE PATHS planned for routing automatically guided vehicles (AGV's) around factories or offices generally comprise a concatenation of line and circular arc segments. For most types of AGV's, the steering functions required to keep the position and heading of the cart continuously aligned with such paths will have discontinuities at the line-arc-line transition points, where the curvature of the path is discontinuous. Since all AGV's have inertia and limited steering forces, these steering discontinuities result in tracking errors, which through proper error sensing and feedback control can be made transient in nature. If the obstacle clearances and docking tolerances are sufficiently large, these transient errors may be of no consequence. However, as the clearances between obstacles or the docking-error tolances become smaller, methods for reducing these tracking errors by eliminating the steering discontinuities become important. This paper discusses three approaches for eliminating steering discontinuities: 1) changing the steering mechanism on the cart, 2) changing the guidepoint on the cart, and 3) changing the curves on the path.

Manuscript received May 5, 1988; revised December 2, 1988.
The author is with AT&T Bell Laboratories, Murray Hill, NJ 07974.
IEEE Log Number 8928449.

The first approach involves choosing a cart with a steering mechanism for which the translational motion is independent of the orientation, i.e., the cart can move in any direction without turning. Two such types are "synchro-drive" vehicles [1] and carts with "Ilonator" wheels [2]. For the "synchro-drive" type of vehicle, all the wheels remain parallel as they turn continuously through the change of angle required by the curved segments of the path. For constant speed motion through a circular arc, the wheels simply make a linear change of angle from the intitial to the final angle of the arc. If the speed divided by the arc radius is less than the angular velocity limit of the steering mechanism, the cart should be able to track the arc segment with negligible error.

The second type of vehicle achieves steering without orientation change through independent control of the rotation of the four "Ilonator" wheels, which have rollers mounted around their circumference, inclined at 45° with respect to the wheel axis. Tracking of a circular arc segment is achieved by continuous speed-control functions to each wheel. This type of vehicle should therefore also have negligible error transients, provided the control and drive systems are properly engineered.

Carts with this omni-directional motion capability not only have the advantage of continuous steering functions, but they also have good docking maneuverability. Yet, most of the robot carts in use or in development today are steered by a single wheel (or wheel pair) [3], [4], [5], or are steered by differentially driven wheels [6], [7], [8]. Both of these more common types of steering have steering discontinuities for ideal path following along line-arc segments. The steered-wheel configuration has discontinuities in the desired steering angle, whereas the differential-drive configuration has discontinuities in the desired velocities of the drive wheels. Section II discusses the elimination of steering discontinuites by changing the guidepoint, and Section III discusses their elimination by changing the type of curves used for the path.

II. Change of Guidepoint

The guidepoint is the point on the robot cart that is designated to follow the reference path. The choice of guidepoint may be somewhat arbitrary, yet its choice affects the space swept out by the cart, the kinematics and dynamics of the cart, and the desired steering and drive functions (the inverse kinematics) for path following. Hence, both the path planning and the path guidance algorithms are affected by the choice of guidepoint. For our experimental cart "Blanche" [3], [9], which is a steered-wheel type, the guidepoint was

0278-0046/89/0800-0330$01.00

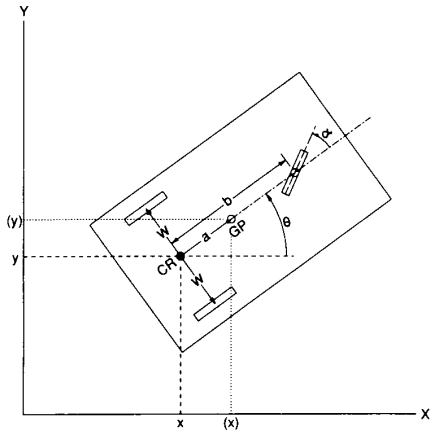

Fig. 1. Steered-wheel cart configuration and workspace coordinates. For the examples in Figs. 2-5, the dimensions are: $b = 24$, $R = 4$, and $W = 10$ in.

chosen at the center of rotation (CR) point midway between the rear wheels. This point was picked mainly for reasons of 1) path planning, since the "shadow" swept by the cart during turns is geometrically simple [10], and 2) maneuverability, since the cart heading is aligned with the path at the end of each turn, and it has the smallest turn radius for a given limit on the steering angle. These factors will be discussed further, once the kinematic relations have been established. Attention is given to both the steered-wheel and the differential-drive configurations in order to show the corresponding effects on the steering and drive functions for these common types of AGV's.

A. Cart Coordinates and Kinematics

The wheel configuration and coordinate system for a steered-wheel tricycle cart are shown in Fig. 1. The coordinates by which the cart is controlled are the front wheel steering angle α and drive velocity ω. With the guidepoint of the cart located at the center of rotation of the cart heading (the point marked "CR" in Fig. 1), the speed v, heading θ, and position (x, y) of the cart are related to the steering angle and drive angular velocity coordinates (α, ω) by the kinematic equations

$$v = R\omega \cos \alpha, \quad \dot{\theta} = (R/b)\omega \sin \alpha$$
$$\dot{x} = v \cos \theta, \qquad \dot{y} = v \sin \theta \tag{1}$$

where R is the radius of the drive wheel, and b is the wheelbase, as shown in Fig. 1. Also shown in parentheses in Fig. 1 are the cart (x, y) coordinates, which would be controlled to follow the path if the guidepoint were moved forward a distance a to the point marked "GP."

Let α_r and ω_r denote the reference steering angle and drive velocity, respectively, required to keep the CR guidepoint moving along the path at a reference speed V. If κ is the *curvature* of the path at the current location of the CR guidepoint, then

$$\alpha_r = \tan^{-1}(b\kappa), \quad \omega_r = V/R \cos \alpha_r). \tag{2}$$

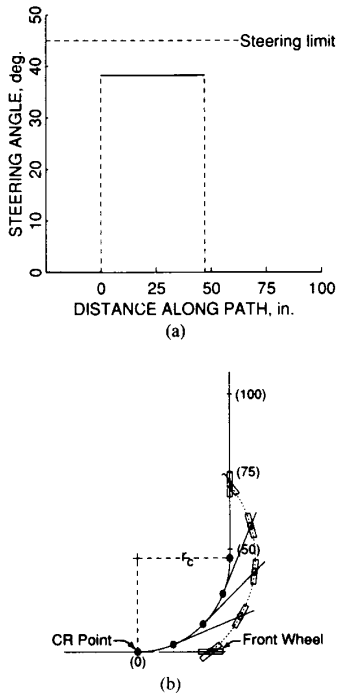

Fig. 2. (a) Steering angle versus distance along the path for a steered-wheel cart with CR point tracking a line-arc-line path with $r_c = 30$ in. The steering limit $\alpha_{max} = 45°$ is shown by the dashed line. (b) CR point and front wheel trajectories. The numbers in parentheses are the distances along the path in inches.

Since the path curvature is zero on line segments and equals $\pm 1/r_c$ on arc segments (where r_c is the radius of the arc, and the sign is positive for CCW and negative for CW turns), it follows from (2) that for the CR point to follow paths of line-arc-line segments, such as shown in Fig. 2, the reference steering function will have two discontinuites, as indicated in Fig. 2(a). As the CR guidepoint moves along the arc segment, the front wheel moves along the dotted arc segment shown in Fig. 2(b). Note that as the CR point follows the path, the cart heading is continuously aligned with the tangent to the arc, so that when the front wheel completes the turn, the cart heading is aligned with the new line segment. If the maximum steering angle for the cart is α_{max}, the smallest radius arc that can be maneuvered by the cart is

$$r_{1\,n} = b/\tan \alpha_{max}. \tag{3}$$

For a differental-drive cart, consider the front wheel in Fig. 1 to be a passive (caster) wheel and the two rear wheels[1] to be driven by separate motors. If the guidepoint is at the CR point $(a = 0)$, the velocity V along the path and the rate of change of cart heading $\dot{\theta}$ are

$$V = (V_R + V_L)/2, \quad \dot{\theta} = (V_R - V_L)/2W \tag{4}$$

where V_R and V_L are the linear velocities of the right and left drive wheels, and W is the distance of each drive wheel from the CR point (see Fig. 1).

[1] Many differential-drive carts have drive wheels located at the middle of the cart (see e.g., [6]-[8]), but the kinematic relations given here still hold.

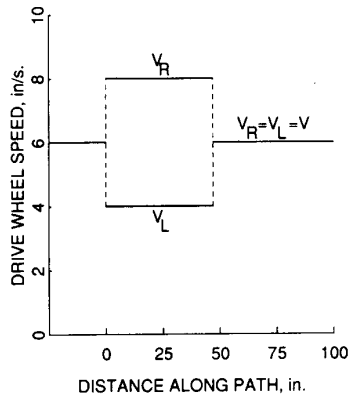

Fig. 3. Drive-wheel velocities versus distance along the path for the CR point of a differential-drive cart tracking the line-arc-line path shown in Fig. 2(b). The CR point moves along the path at 6 in/s.

For the CR point on the differential drive cart to follow a path at a speed V, the left and right drive wheel velocities must be

$$V_L = V(1 - W\kappa), \quad V_R = V(1 + W\kappa) \tag{5}$$

where κ is the curvature of the path. As described below (2), the curvature on paths made up of lines and circular arcs is zero or $\pm 1/r_c$, respectively. Therefore, the wheel velocities required for the CR point to follow the path shown in Fig. 2(b) will have $\pm VW/r_c$ discontinuities, as indicated in Fig. 3.

B. Shifted Guidepoint Kinematics

If the guidepoint for the steered-wheel cart is shifted forward of the CR point along the cart axis by a distance a to the point marked GP in Fig. 1, the (x, y) workspace coordinates are translated by $(a \cos\theta, a \sin\theta)$. The kinematic equations for the x and y velocities at the new guidepoint become:

$$\dot{x} = R\omega\left(\cos\alpha\cos\theta - \frac{a}{b}\sin\alpha\sin\theta\right), \qquad \dot{y} = R\omega\left(\cos\alpha\sin\theta + \frac{a}{b}\sin\alpha\cos\theta\right) \tag{6}$$

where the heading θ is determined by integrating the expression for $\dot{\theta}$ in (1).

When the shifted guidepoint is tracking a path, explicit expressions like those in (2) for the inverse kinematic functions α_r and ω_r are not available. The reference steering angle and drive velocity must now be obtained from (6) by numerical integration methods. As noted by Graettinger and Krogh [11], if the guidepoint is at the center of mass and not at the CR point, the required steering function for tracking a line-arc path no longer has the discontinuities shown in Fig. 2(a). This is due to the fact that the cart heading is no longer required to be tangent to the arc at all times, as it was when the CR point was tracking the arc. The result will be illustrated for the interesting case in which the guidepoint is shifted to the front wheel, that is, where $a = b$.

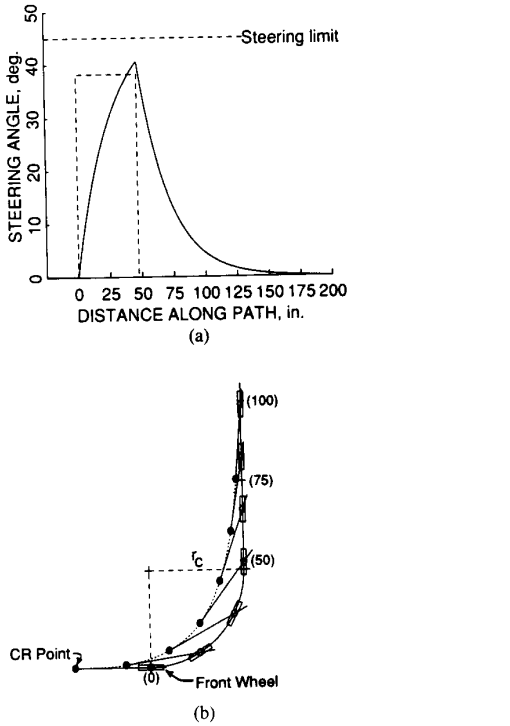

Fig. 4. (a) Steering function (solid curve) with front-wheel tracking of a line-arc-line path with arc radius r_c = 30 in. The dashed line is the steering function for CR point tracking (Fig. 2). (b) Front wheel and CR-point trajectories. The numbers in parentheses are the distances along the path in inches.

When the front wheel is designated as the guidepoint, the kinematic equations for the x and y velocities become (using $a = b$ in (6))

$$\dot{x} = R\omega\cos(\alpha + \theta), \quad \dot{y} = R\omega\sin(\alpha + \theta) \tag{7}$$

where, as before, the heading θ is determined by integrating the $\dot{\theta}$ in (1). Since the front wheel now tracks the path, the drive velocity ω_r, required to move this guidepoint at the reference velocity V, is simple V/R. The reference steering function α_r, which keeps the front wheel on the arc segment of radius r_c, is the solution of the nonlinear differential equation

$$\dot{\alpha}_r + (V/b)\sin\alpha_r = V/r_c, \quad \alpha_r(0) = 0. \tag{8}$$

The numerical integration of (7) and (8) matching the boundary conditions for the line-arc-line left-turn path shown in Fig. 2(a) yields the continuous steering function for front-wheel path tracking shown in Fig. 4(a). For comparison, the discontinuous steering function for the CR point tracking of this path (Fig. 2) is shown in dashed lines.

So the good news is that merely by shifting the guidepoint that tracks the path, we can eliminate the discontinuities in the steering function for the steered-wheel cart. The bad news is that the cart can no longer maneuver through as sharp a turn as when the CR point tracks the path (for the same steering-angle limit α_{max}), and the heading of the cart is not aligned with the path following a turn until a considerable distance has been traversed along the new straight-line segment. As indicated in

Fig. 4(a), the peak steering angle for the shifted guidepoint steering function exceeds the constant steering angle for CR-point tracking of the same arc. If the arc had the minimum radius given by (3), the shifted guidepoint steering function would therefore exceed the steering-angle limit α_{max}.

The heading misalignment problem is illustrated in Fig. 4(b), where the trajectory of the CR point as the front wheel tracks the line-arc-line path is plotted. The cart heading is indicated by the sequence of tangents to the CR trajectory. Note that after the turn, several cart-lengths are required before the cart heading is reasonably well aligned with the new path heading. If a parallel docking point occurs shortly after such a turn, the cart may have to be programmed to make correcting maneuvers in order to properly dock. The path-planning algorithm also may become much more complex because of these factors. For many applications where steered-wheel AGV's are to be used, it may therefore be advantageous to keep the guidepoint at the CR point of the cart.

For the differential-drive type of cart, if the guidepoint is shifted a distance a from the CR point, the kinematic relations for the x to y velocities of the guidepoint path, as a function of the CR point velocity V and rate of change of cart heading $\dot{\theta}$, are

$$\dot{x} = V\cos\theta - a\dot{\theta}\sin\theta, \quad \dot{y} = V\sin\theta + a\dot{\theta}\cos\theta. \tag{9}$$

The CR point velocity V and rate of change of cart heading $\dot{\theta}$ are, in turn, functions of the drive wheel velocities V_R and V_L, as given in (4).

Conversely, if the guidepoint is following a specified path at a given speed, from (9), the CR point velocity V and heading rate $\dot{\theta}$ can be written in terms of the known path velocities $\dot{x}$ and $\dot{y}$ and heading θ as

$$V = \dot{x}\cos\theta + \dot{y}\sin\theta, \quad \dot{\theta} = (\dot{y}\cos\theta - \dot{x}\sin\theta)/a. \tag{10}$$

The shifted guidepoint drive wheel velocities for a given path can be derived by numerical integration of $\dot{\theta}$ in (10) and using the values of θ to derive V, also given in (10). Then, from (4), the left and right drive wheel velocities are given by

$$V_L = V - W\dot{\theta}, \quad V_R = V + W\dot{\theta}. \tag{11}$$

Though not apparent from these expressions, the drive wheel velocities that cause the shifted guidepoint to follow line-arc paths are continuous functions. As an example, consider again the line-arc-line path shown in Fig. 2(b). If the guidepoint is shifted from the CR point by a distance $a = 10$ in. (see Fig. 1), for the guidepoint following the path at a constant speed of 6 in/s, the drive-wheel velocities have the form shown in Fig. 5(a).

In Fig. 5(b) the trajectories followed by the guidepoint (GP) and the center of rotation (CR) of the differential-drive cart are shown. The CR point moves inside the path the GP follows, and the cart heading is not realigned with the path until the cart has moved some distance along the second line segment. However, since a differential-drive cart can correct its heading while stopped and can track very small radius arcs at reduced speeds, it is not likely that much, if any, maneuverability is lost.

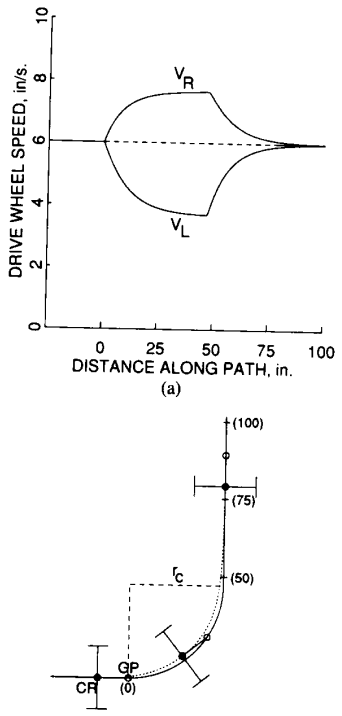

Fig. 5. (a) Drive wheel velocities for a differential-drive cart with shifted guidepoint, $a = 10$ in. The guidepoint moves along the path at 6 in/s. (b) CR and guidepoint (GP) trajectories. Numbers in parentheses are the distances along the path in inches.

III. Change Of Curve Type

Although arcs of circles are convenient for the curved portions of paths and in some cases are optimal for constructing minimum distance paths [12], they are not the only type of curves that should be considered in generating paths for robot carts. As discussed in the previous sections, curves having zero curvature at their end points are one of the ways to avoid AGV steering-function discontinuities. It was shown in Section II-A that when the guidepoint is located at the CR point of the cart (see Fig. 1), the reference steering angle given in (2) for the steered-wheel-type cart and the reference drive velocities (5) for the differential-drive type cart are directly proportional to the path curvature κ. Therefore, if it is desirable to keep the guidepoint at the CR point, the only way to avoid steering discontinuities for either of these cart configurations is to provide continuous-curvature paths for them to follow.

One type of curve that has been used for continuous-curvature path generation is a "clothoid" curve segment. A clothoid or Cornu spiral [13] is a curve whose curvature is a linear function of distance along the curve, starting at zero. Kanayama and Miyake [7] use a "clothoid pair" to make curves with zero curvature at their junctures with line segments in order to produce continuous drive-velocity functions for a differential-drive cart. Clothoid pair curves have the advantage of providing the minimum-length continuous-curvature paths for a given limit on curvature rate or centripetal jerk [14]. Clothoid pairs have the disadvantage,

however, that the (x, y) coordinates of the curve have no closed-form expressions but must be derived by integrating along the path length s with the curvature $\kappa(s)$ linearly increasing from zero during the first half of the turn, then linearly decreasing to zero during the second half, in such a way that the end-point of the curve precisely matches the position and slope constraints of the succeeding line segment. Any errors in the slope of the curvature function, or in the numerical integration routine, may result in a mismatch of these end-point conditions.

In this section, we describe, as alternatives to segments like the clothoid-pair whose curvatures are defined as a function of path-length, two different types of curves. Both have closed-form expressions that match *a priori* the boundary conditions of the two lines they join. The first is a cartesian quintic polynomial [15], which is particularly appropriate for producting continuous-curvature lane-change paths. The second curve is a polar coordinate polynomial, called a "polar spline" [15][2], which can be used to produce continuous-curvature paths for symmetric turns of arbitrary angle.

A third type of curve, called a "super-arc," [16] can be used for generating continuous-curvature paths whose turns consist entirely of right-angle turns, but since it has no significant advantage over the polar spline for such turns, it is not considered further here.

A. Quintic Polynomial Paths

Curves that produce a transition between parallel lanes in the same direction will be called lane-change maneuvers. The "lazy-S" type curves needed for such maneuvers are typically constructed out of two arc segments or an arc-line-arc sequence. These multiple segment paths can be replaced by a single quintic polynomial segment that provides a continuous-curvature transition between the parallel lanes of travel.

The general expression for a quintic polynomial in cartesian coordinates is

$$y(x) = a_0 + a_1 x + a_2 x^2 + a_3 x^3 + a_4 x^4 + a_5 x^5. \quad (12)$$

Consider the lane-change maneuver in the coordinate frame shown in Fig. 6(a). The six coefficients in (12) are chosen to satisfy the position, slope, and curvature constraints of this maneuver, namely

$$y = 0, \quad \frac{dy}{dx} = 0, \quad \kappa = 0 \quad \text{at } x = 0$$

$$y = y_e, \quad \frac{dy}{dx} = 0, \quad \kappa = 0 \quad \text{at } x = x_e \quad (13)$$

where κ is the curvature of $y(x)$, given by

$$\kappa = (d^2y/dx^2)/[1 + (dy/dx)^2]^{3/2}.$$

[2] The term "spline," as currently used in graphics and data smoothing literature (see e.g., C. de Boor, *A Practical Guide to Splines*, Springer (1978)), implies using a *sequence* of polynomials, rather than a single polynomial. However, we use (and hopefully not abuse) the term in the older, broader sense of curves providing suitably smooth transitions between lines or points, such as the curves produced by bending thin wood or metal strips.

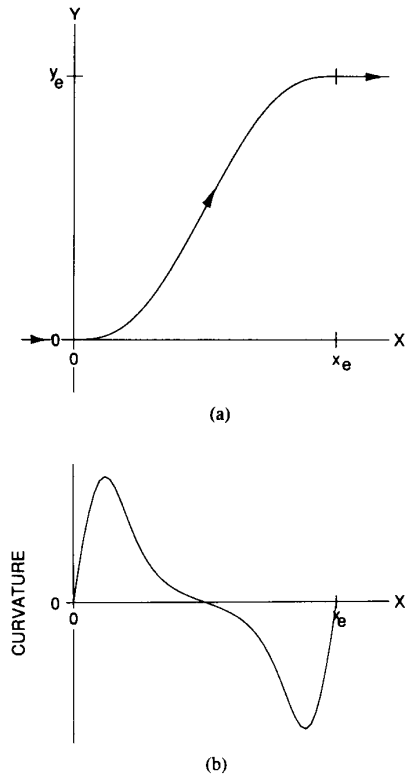

Fig. 6. (a) Lane-change maneuver using a quintic polynomial segment; (b) curvature function of the quintic polynomial.

The quintic polynomial satisfying the constraints (13) has only three nonzero coefficients and can be written in the form

$$y(x) = y_e \left[10 \left(\frac{x}{x_e}\right)^3 - 15 \left(\frac{x}{x_e}\right)^4 + 6 \left(\frac{x}{x_e}\right)^5 \right]. \quad (14)$$

The quintic polynomial curve resulting from (14) is shown in Fig. 6(a). The curvature function, shown in Fig. 6(b), shows that the quintic polynomial provides the desired continuous curvature path. The maximum curvature and curvature-rate for the function shown in Fig. 6(b) increase directly with the lane-change slope ratio y_e/x_e. This ratio must be chosen sufficiently low so that the resulting continuous steering function does not violate the peak steering and steering-rate constraints for a particular AGV design. Given that these constraints are met, the simple three-term expression (14) for the quintic polynomial applies to lane-change segments of arbitrary location and orientation in the workspace layout by transforming from the coordinate frame shown in Fig. 6(a) to the coordinate frame aligned with the lane-change starting point.

B. Polar Spline Paths

Curves that produce a smooth transition between lines intersecting at an arbitrary angle, and are symmetric with respect to the intersection point, will be called "arc turns." The turn angle is measured in the direction of the change of heading with counter-clockwise positive.

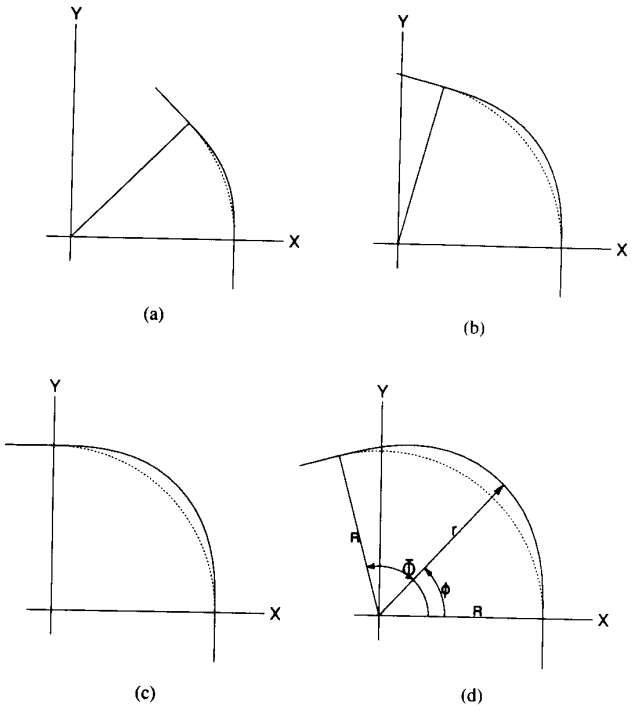

Fig. 7. Polar spline segments for arc turns of (a) 45, (b) 75, (c) 90, and (d) 105°. The corresponding circular arc turns are shown as dotted lines.

A cartesian quintic polynomial, given by (12), can be used to provide continuous-curvature turns that are close in shape to arc turns, provided the magnitude of the turn angle is less than about 45°. For larger angles, however, the quintic begins to curve away from the circular arc and "blows up," i.e., has coefficients tending to infinity, as the turn angle approaches 90° [15]. This problem could be avoided by segmenting a large-angle turn into several smaller turns, but a concatenation of curve segments requires additional computation that we would like to avoid.

What we would like to have is a single, smooth curve segment that does not deviate too far in shape from the circular arc it will replace and yet can satisfy the position, heading, and curvature constraints imposed at the start and end points. To achieve this, the coordinates of the curve should be chosen so that the independant variable changes relatively uniformly with respect to the distance along the curve, regardless of the total angle. It seems appropriate, therefore, to consider polar coordinates, with the curve specified by the polar length r, as a function of the polar angle ϕ. The curve $r(\phi)$, expressed as a polynomial in ϕ, has the general form

$$r(\phi) = a_0 + a_1\phi + a_2\phi^2 + a_3\phi^3 + a_4\phi^4 + \cdots \tag{15}$$

where the number of terms needed depends on the number of conditions imposed.

Consider arc turns in the coordinate frame shown in Fig. 7. Here, R is the radius of the circular arc connecting the two line segments, and Φ is the total angle of the turn. The position, slope, and curvature constraints on the polynomial (15) for the desired arc turns are

$$\begin{aligned} &r = R, \quad r' = 0, \quad \kappa = 0 \quad \text{at } \phi = 0 \\ &r = R, \quad r' = 0, \quad \kappa = 0 \quad \text{at } \phi = \Phi \end{aligned} \tag{16}$$

where $r' \equiv dr/d\phi$, and κ is the curvature of r. The general expression for curvature of any curve is

$$\kappa = d\theta/ds \tag{17}$$

where s is the distance along the path, and θ is the angle of the tangent to the path (also the *heading* of a vehicle whose CR point is following the path).

For a path defined in polar coordinates (r, ϕ), the tangent angle can be expressed as

$$\theta = \pi/2 + \phi - \tan^{-1}(r'/r).$$

Differentiating this with respect to ϕ gives

$$\frac{d\theta}{d\phi} = 1 - \frac{rr'' - 2r'^2}{r^2 + r'^2} \tag{18}$$

where $r'' \equiv d^2r/d\phi^2$.

The infinitesimal change in path length ds is given in polar form by

$$ds = (r^2 + r'^2)^{1/2} d\phi. \tag{19}$$

Using (18) and (19) in (17) yields the desired expression for the curvature, namely

$$\kappa = \frac{r^2 + 2r'^2 - rr''}{(r^2 + r'^2)^{3/2}}. \tag{20}$$

Using the position and slope constraints of (16) in (20), it follows that the zero curvature constraints in (16) are equivalent to requiring that $r'' = R$ at $\phi = 0$ and $\phi = \Phi$. Applying these constraints on r, r', and r'' yields four nonzero coefficients in (15), namely: $a_0 = R$, $a_2 = R/2$, $a_3 = -R/\Phi$, and $a_4 = R/2\Phi^2$. This polar spline fit between line segments can thus be written as

$$r(\phi) = R\left(1 + \frac{\phi^2}{2} - \frac{\phi^3}{\Phi} + \frac{\phi^4}{2\Phi^2}\right). \tag{21}$$

The (x, y) coordinates of the polar spline are then obtained from $x = r\cos\phi$ and $y = r\sin\phi$.

The continuous-curvature polar splines resulting from (21) are shown in Fig. 7 for four values of the turn angle Φ. The curvature functions (20) for these four polar spline segments are shown in Fig. 8. The paths and curvature functions for the corresponding circular arc turns are also shown (dashed lines) for comparison. For turn angles of 90° or less, the polar spline curvature functions are very close to parabolic in shape and are very close to the "cubic spiral" curves of Kanayama and Hartman [17], which are optimally-smooth curves, in the sense of minimizing the integral-square-curvature rate (centripetal jerk). In this sense, the single-segment polar splines provide a simple means to achieve near-optimally smooth arc turns of 90° or less.

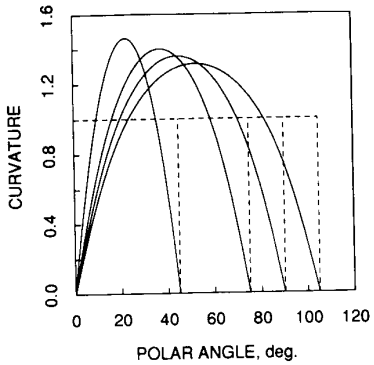

Fig. 8. Curvature functions for the polar spline segments of Fig. 7. The curvature functions for the corresponding circular arcs are shown in dashed lines.

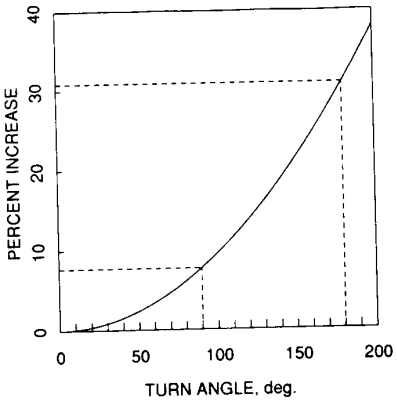

Fig. 9. Percent increase in peak radial length for single-segment polar splines as compared to circular arc turns as a function of turn angle.

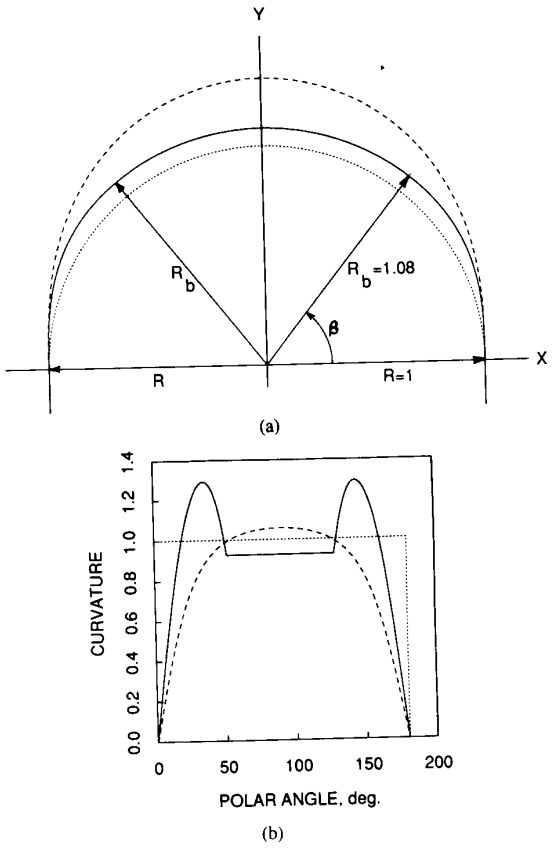

Fig. 10. (a) Three-segment polar spline (solid line) for a 180° turn, compared with a single-segment polar spline (dashed line) and a circular arc (dotted). (b) Curvature functions for the curves in (a).

These results suggest that the polar spline is a very appropriate choice for producing continuous-curvature arc turns of arbitrary angle. It has a closed-form expression (21), which is a simple function of the turn radius R and turn angle Φ. The curve it produces is symmetric, has near-optimal smoothness in the sense described above, and is reasonably close to the circular arc, although both these qualities begin to degrade for turn angles greater than 90°.

The peak value r_p of $r(\phi)$ in (21) occurs at the mid-point of the turn, where $\phi = \Phi/2$. The ratio of this peak value to the radius of the circular arc is thus given by

$$\frac{r_p}{R} = 1 + \frac{\Phi^2}{32} \tag{22}$$

where Φ is the turn angle in radians. The second term in (22), which represents the fractional increase in the peak value of the polar spline radial over that of the circular arc, is plotted in Fig. 9 for turn angles up to 200°. For right-angle turns, the increase is only about 8 percent, but it grows as the square of the turn angle, and for 180° turns, it is over 30 percent.

If turn angles greater than 90° are needed in a path layout and if the workspace clearances are too small for the wider path swept out by the single-segment polar spline, the path designer can use a three-segment polar spline [14], which follows the circular arc turn more closely, at the expense of increased peak curvature and curvature rate. This three-segment polar spline is discussed in detail in the cited reference and will only be illustrated here by the example for a 180° turn shown in Fig. 10(a). The knots for the segments of this polar spline occur at the polar angles 0, β, $\pi - \beta$, and π, where $\beta = 51.6°$ in this example. Note that the three-segment spline (solid line) has only an 8-percent increase in radial length over the circular arc (dotted), as compared to the 31-percent increase for the one-segment spline (dashed line). The curvature functions, plotted in Fig. 10(b), show that this closer tracking of the circular-arc turn is achieved at a cost of more than a 20-percent increase in peak curvature.

IV. Conclusions

For the three approaches for avoiding steering discontinuities discussed in this paper, the following conclusions are suggested:

1) If omni-directional carts such as those using the "synchro-drive" [1] or "Ilonator" [2] configurations can meet the cost, performance, and reliability requirements of the particular AGV application, they should be chosen. Not only are they free of the steering discontinuity problem that the more common steered-wheel and differential-drive carts have, but they also have an overall maneuverability superior to that of either the differential-drive cart or the steered-wheel cart.

However, if the choice is restricted to the latter two configurations, the differential-drive seems preferable to the steered-wheel configuration, at least in terms of maneuverability.

2) The elimination of steering discontinuities by shifting the guidepoint, discussed in Section II, may be a reasonable option for differential-drive carts, particularly if the center-of-rotation (CR) point between the drive wheels is not co-located with the center of mass or some other critical guidepoint. It is probably a less attractive option for steered-wheel carts because of the misalignment of the cart heading at the end of turns. For example, if the guidepoint is shifted so that the front wheel tracks the path, several cart lengths on the straight-line path following a right-angle turn are required before the cart heading is reasonably well aligned with the path. Accurate docking thus may not be possible without either long, straight approarch-segments or back-up maneuvers, which makes for more complicated and lengthy paths.

3) The option of eliminating steering discontinuities by generating continuous-curvature paths, discussed in Section III, is a reasonable one for both steered-wheel and differential-drive carts, particularly when it is desirable to keep the guidepoint at the CR point of the cart. Of the proposed replacements for circular-arc segments in line-arc paths, the polar spline is the most suitable for arc turns of arbitrary angle. The cartesian quintic polynomial, however, is an attractive candidate for continuous-curvature lane-change segments on the path since it generates the complete maneuver with a single segment. Both curves have the advantage over path-length parametric curves, such as the clothoid, in that they have a closed-form expression that guarantees precise matching of the two-point boundary conditions, and they require only slightly more geometric computation than that required for the circular arc segments.

The continuous steering-function constraint is, of course, not the only constraint that may be needed in order to generate feasible paths for AGV's to follow. However, the other dynamic and kinematic constraints may usually be satisfied by applying the appropriate time-scaling, or speed adjustment, to critical segments of the path [11].

References

[1] J. M. Holland, "A mobile platform for industrial research," SME Robotics Research Conf., Scottsdale, AZ, Soc. Manuf. Engrs. Tech Paper MS86-786, 1986.

[2] B. E. Ilon, "Wheels for a course stable self-propelling vehicle movable in any desired direction on the ground or some other base," U.S. Patent No. 3 876 255 (1975).

[3] I. J. Cox, "Blanche: An autonomous robot vehicle for structured environments," in *Proc. 1988 IEEE Int. Conf. Robotics Automation* (Philadelphia, PA).

[4] M. Julliere, L. Marce, and H. Perrichot, "A guidance system for a vehicle which has to follow a memorized path," in *Proc. 2nd Int. Conf. Automated Guided Vehicle Syst. 16th IPA Conf., H. J. Warnecke, ed.,* New York: North Holland Publ. Co., 1983, p. 195.

[5] K. Komoriya, S. Tachi, and K. Tanie, "A method of automomous locomotion for mobile robots," *Advanced Robotics,* vol. 1, no. 1, pp. 3-19, 1986.

[6] S. K. Premi and C. B. Besant, "A review of various vehicle guidance techniques that can be used by mobile robots or AGV's," in *Proc. 2nd Int. Conf. Automated Guided Vehicle Syst. 16th IPA Conf.,* H. J. Warnecke, ed., New York: North Holland Publ. Co., 1983, p. 195.

[7] Y. Kanayama and N. Miyake, "Trajectory generation for mobile robots," in *Proc. 3rd Int. Symp. Robotics Research,* O. D. Faugeras and G. Giralt, Eds. (Gouvieux, France), 1985, pp. 333-340.

[8] T. Hongo, H. Arakawa, G. Sugimoto, K. Tange, and Y. Yamamoto "An automatic guidance system of a self-controlled vehicle," *IEEE Trans. Ind. Electron.,* vol. IE-34, no. 1, pp. 5-10, 1987.

[9] W. L. Nelson and I. J. Cox, "Local path control for an autonomous vehicle," in *Proc. 1988 IEEE Int. Conf. Robotics and Automation* (Philadelphia, PA).

[10] G. T. Wilfong, "A path planning algorithm for a mobile robot cart," in *Proc. 1988 IEEE Int. Conf. Robotics and Automation,* (Philadelphia, PA).

[11] T. J. Graettinger and B. H. Krogh, "Evaluation and time-scaling of trajectories for wheeled mobile robots," Carnegie Mellon U., Dept. Electrical & Computer Engineering Report dated 27 Nov. 1987, to appear in *ASME J. of Dynamic Systems, Meas. & Control,* 1989.

[12] L. E. Dubins, "On curves of minimal length with a constraint on average curvature and with prescribed initial and terminal positions and tangents," *Amer. J. Math.,* vol. 79, pp. 497-516, 1957.

[13] R. C. Yates, *Curves and Properties.* Goshen, NY: Classics Publishing Co., 1952.

[14] W. L. Nelson, "Continuous-curvature paths for autonomous vehicles," *Proc. 1989 IEEE Int. Conf. Robotics Automation* (Scottsdale, AZ).

[15] W. L. Nelson, "Continuous-curvature paths using quintic and polar splines," AT&T Bell Labs internal document, Mar. 1988.

[16] W. L. Nelson, "Continuous steering function control of a robot cart," AT&T Bell Labs internal document, Oct. 1987.

[17] Y. Kanayama and B. Hartman, "Smooth local path planning for autonomous vehicles," Univ. of California, Santa Barbara, Tech. Report TRCS88-15, 1988.